

H_∞ DESIGN OF CONTROLLERS ENSURING THE REGULATION OF CURRENTS OF THE DECOUPLED FIELD ORIENTATION CONTROL APPLIED TO A PMS MOTOR

Ahmed AZAIZ*, Youcef RAMDANI**, Abdelkader MEROUFEL**, Baghdad BELABBES**

*Department of Electronics, Faculty of Sciences of the engineer, University of Sidi Bel Abbes Algeria E-mail: azaiz_ah@yahoo.fr,

**Department of Electrical Engineering, Faculty of Sciences of the engineer, University of Sidi Bel Abbes Algeria, E-mail: ramdaniy@yahoo.fr

ABSTRACT

The dynamics neglected during the identification of the process, the variation of stator resistances and cyclic inductances induce a difference between the process and the nominal mathematical model.

These drifts are due to the temperature, the saturation of the magnetic circuit and the skin effect. In this case, the traditional methods such as Bode design, Nyquist design, and Nichols chart design fail to satisfy robust stability and performance. To solve this problem, an efficient robust method called the H_∞ design method is used. This approach permits to achieve a successfully designed control system, which is able to maintain stability and performance level in spite of uncertainties in system dynamics. In this article, we present the field orientation control (FOC) of the permanent magnets synchronous machine (PMSM) fed by a voltage source inverter with regulated currents on the d and q axes.

The field orientation control consists in regulating the flux by one component of the current and the torque by the other component. So, it is necessary to consider a reference frame attached to the rotor with direct and quadrature axes and a control law that ensure the decoupling of the torque and flux. In the case of the permanent magnets synchronous machine, if the current i_d is maintained null, the stator reaction flux is in quadrature with the flux produced by the permanent magnets, then the torque becomes directly proportional to the current i_q and the model of the machine becomes equivalent to that of the DC machine. As a result, the model of the PMS machine is divided into two independent SISO systems.

Keywords: stabilisable, detectable, spectral radius, singular value, infinity norm, uncertainty, robustness.

1. INTRODUCTION

A PID controller is designed to control the rotor speed. It delivers the reference current i_{qr} . Two H_∞ optimal controllers are designed, one controls the current i_q and the other controls the current i_d . To design the H_∞ optimal controllers, we use the state-space approach to solve a standard H_∞ problem [8, 9, 10, 11], which is to find an output feedback controller K(s) so that the H_∞ norm of the closed-loop transfer function is strictly less than a prescribed positive number γ :

$$\|T_{zw}\|_{\infty} < \gamma \quad (1)$$

The existence of the controller depends upon the unique stabilizing solutions to two algebraic Riccati equations being positive semi definite and the spectral radius of their product being less than γ^2 . The feedback configuration is shown in Fig.1, where P(s) is a linear system described by the following state space equation:

$$\begin{aligned} \dot{x}(t) &= A x(t) + B_1 w(t) + B_2 u(t) \\ z(t) &= C_1 x(t) + D_{11} w(t) + D_{12} u(t) \\ y(t) &= C_2 x(t) + D_{21} w(t) + D_{22} u(t) \end{aligned} \quad (2)$$

where $x(t) \in R^n$ is the state vector, $w(t) \in R^{m_1}$ the exogenous input vector, $u(t) \in R^{m_2}$ the control input vector, $z(t) \in R^{p_1}$ the error (output) vector, and $y(t) \in R^{p_2}$ the measurement vector.

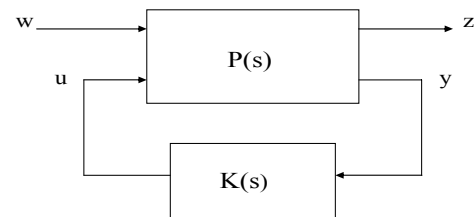


Fig. 1 A feedback system.

The results are obtained under the following assumptions:

A1 (A, B_2) is stabilisable and (A, C_2) is detectable;

A2 $D_{12} = \begin{bmatrix} 0 \\ I_{m_2} \end{bmatrix}$ and $D_{21} = \begin{bmatrix} 0 & I_{p_2} \end{bmatrix}$

A3 $\begin{bmatrix} A - j\omega I & B_2 \\ C_1 & D_{12} \end{bmatrix}$ has full column rank for all ω ;

A4 $\begin{bmatrix} A - j\omega I & B_1 \\ C_2 & D_{21} \end{bmatrix}$ has full row rank for all ω .

2. THE PMS MACHINE MODEL

The model of the PMS machine can be described by the following equations expressed in the rotor reference frame (qd frame):

$$v_d = r_s i_d + L_d \frac{di_d}{dt} - \omega L_q i_q \quad (3)$$

$$v_q = r_s i_q + L_q \frac{d i_q}{dt} + \omega L_d i_d + \omega \phi_f \quad (4)$$

$$T_e = \frac{3}{2} p (\phi_f i_q + (L_d - L_q) i_d i_q) \quad (5)$$

$$\omega = p \omega_r$$

The mechanical equation is given by

$$J \frac{d\omega_r}{dt} = T_e - F \omega_r - T_m \quad (6)$$

$$\omega_r = \frac{d\theta}{dt} \quad (7)$$

To have the two axes d and q decoupled, the terms $\omega L_q i_q$ and $(\omega L_d i_d + \phi_f)$ are neglected from the expressions (3) and (4), respectively. The model of the machine becomes:

$$v_{d0} = r_s i_d + L_d \frac{d i_d}{dt} \quad (8)$$

$$v_{q0} = r_s i_q + L_q \frac{d i_q}{dt} \quad (9)$$

Each coupling term is added to the output signal of the corresponding current controller ($K_d(s)$ or $K_q(s)$), in order to obtain the reference voltages v_{dr} and v_{qr} , as shown in Fig.1 and Fig.2.

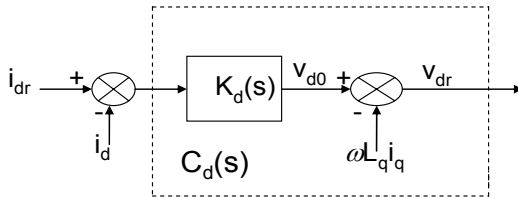


Fig. 2 Reference voltage (v_{dr}) generation

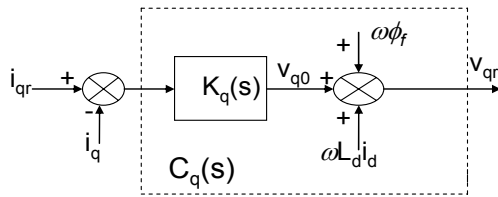


Fig. 3 Reference voltage (v_{qr}) generation.

The entire block diagram representing the field orientation control (FOC) of the PMS machine is shown in Fig. 4.

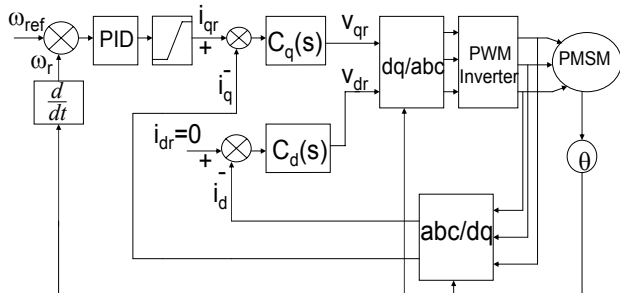


Fig. 4 FOC of the PMS machine

3. H_∞ DESIGN OF CONTROLLERS

3.1. Solution formulae

Theorem 1. [2, 5, 6, 8] With $P(s)$ satisfying the assumptions A1–A4. There exists an internally stabilising controller $K(s)$ such that

$$\|F_L(P, K)\|_{\infty} < \gamma \quad \text{if and only if}$$

$$(a) \max(\bar{\sigma}[D_{1111} \ D_{1112}], \bar{\sigma}([D_{1111}^T \ D_{1121}^T]^T)) < \gamma$$

where $\bar{\sigma}$ denotes the largest singular value of the corresponding matrix,

$$D_{11} = \begin{bmatrix} D_{1111} & D_{1112} \\ D_{1121} & D_{1122} \end{bmatrix}$$

and

(b) there exist stabilising solutions $X \geq 0$ and $Y \geq 0$ satisfying the two algebraic Riccati equations corresponding to the Hamiltonian matrices H and J , respectively, and such that

$$\rho(XY) < \gamma^2$$

where $\rho(\bullet)$ denotes the spectral radius.

The H_∞ solution formulae use solutions of two algebraic Riccati equations.

Let's define

$$B = [B_1 \ B_2] \quad (10)$$

$$C = [C_1^T \ C_2^T]^T \quad (11)$$

$$D_{1s} = [D_{11} \ D_{12}] \quad (12)$$

$$D_{s1} = [D_{11}^T \ D_{21}^T]^T \quad (13)$$

$$R_{nh} = D_{1s}^T D_{1s} - \begin{bmatrix} \gamma^2 I_{m_1} & 0 \\ 0 & 0 \end{bmatrix} \quad (14)$$

$$R_{nj} = D_{s1} D_{s1}^T - \begin{bmatrix} \gamma^2 I_{p_1} & 0 \\ 0 & 0 \end{bmatrix} \quad (15)$$

Assume that R_{nh} and R_{nj} are nonsingular. We define two Hamiltonian matrices H and J as

$$H = \begin{bmatrix} A & 0 \\ -C_1^T C_1 & -A^T \end{bmatrix} - \begin{bmatrix} B \\ -C_1^T D_{1s} \end{bmatrix} R_{nh}^{-1} [D_{1s}^T C_1 \ B^T]$$

$$H = \begin{bmatrix} E_x & -W_x \\ -Q_x & -E_x^T \end{bmatrix} \quad (16)$$

$$J = \begin{bmatrix} A^T & 0 \\ -B_1 B_1^T - A \end{bmatrix} - \begin{bmatrix} C^T \\ -B_1 D_{s1}^T \end{bmatrix} R_{nj}^{-1} [D_{s1} B_1^T \ C]$$

$$J = \begin{bmatrix} E_y & -W_y \\ -Q_y & -E_y^T \end{bmatrix} \quad (17)$$

The stabilising solutions X and Y are symmetric matrices that solve the algebraic Riccati equations (18) and (19) respectively and are such that $E_x - W_x X$ and $E_y - W_y Y$ are stable matrices

$$E_x^T X + X E_x - X W_x X + Q_x = 0 \quad (18)$$

$$E_y^T Y + Y E_y - Y W_y Y + Q_y = 0 \quad (19)$$

Based on X and Y, a state feedback matrix F and an observer gain matrix L can be constructed

$$F = -R_{nh}^{-1} (D_{1s}^T \bar{C}_1 + B^T X) \quad (20)$$

$$F = \begin{bmatrix} F_1 \\ F_2 \end{bmatrix} = \begin{bmatrix} F_{11} \\ F_{12} \\ F_2 \end{bmatrix}$$

$$L = -(B_1 D_{s1}^T - Y C^T) R_n^{-1} \quad (21)$$

$$L = [L_1 \ L_2] = [L_{11} \ L_{12} \ L_2] \quad (22)$$

Theorem 2. [2, 5, 6, 8] Given that the conditions of theorem 1 are satisfied, then all rational, internally stabilising controllers, K(s), satisfying

$$\|F_l(P(s), K(s))\|_{\infty} < \gamma \text{ are given by} \\ K(s) = F_l(M, \Phi)$$

For any rational $\Phi(s) \in \mathcal{H}_{\infty}$ such that $\|\Phi_s\|_{\infty} < \gamma$, where M(s) has the realisation

$$M(s) = \begin{bmatrix} \hat{A} & \hat{B}_1 & \hat{B}_2 \\ \hat{C}_1 & \hat{D}_{11} & \hat{D}_{12} \\ \hat{C}_2 & \hat{D}_{21} & 0 \end{bmatrix} \quad (23)$$

and

$$TD11 = (\gamma^2 I_{p_1 - m_1} - D_{1111} D_{1111}^T)^{-1} D_{1112} \\ \hat{D}_{11} = -D_{1121} D_{1111} TD11 - D_{1122} \quad (24)$$

$$TD12 = (\gamma^2 I_{m_1 - p_2} - D_{1111}^T D_{1111})^{-1} \\ T_1 = I_{m_2} - D_{1112} TD12 D_{1121}^T \quad T_2 = T_1^T \\ \hat{D}_{12} \text{ is the Cholesky factor of } T_2 \quad (25)$$

$$TD21 = (\gamma^2 I_{p_1 - m_2} - D_{1111} D_{1111}^T)^{-1} \\ T_3 = I_{p_2} - D_{1112}^T TD21 D_{1112} \\ \hat{D}_{21} \text{ is the Cholesky factor of } T_3. \quad (26)$$

$$Z = (I - \gamma^{-2} YX)^{-1} \\ \hat{B}_2 = Z(B_2 + L_{12}) \hat{D}_{12} \quad (27)$$

$$\hat{C}_2 = -\hat{D}_{12} (\bar{C}_2 + F_{12}) \quad (28)$$

$$\hat{B}_1 = -Z L_2 + \hat{B}_2 \hat{D}_{12}^{-1} \hat{D}_{11} \quad (29)$$

$$\hat{C}_1 = U_{12} (F_2 + \hat{D}_{11} \hat{D}_{21}^{-1} \hat{C}_2) \quad (30)$$

$$\hat{A} = A + B F + \hat{B}_1 \hat{D}_{21}^{-1} \hat{C}_2 \quad (31)$$

$\Phi(s)$ is chosen to be 0, then the corresponding suboptimal controller called the central controller is given in state-space form:

$$K(s) = \begin{bmatrix} \hat{A} & \hat{B}_1 \\ \hat{C}_1 & \hat{D}_{11} \end{bmatrix} \quad (32)$$

3.2. Selection of weighting filters

The transfer functions of the plants in the d and q axis are derived from equations (8) and (9) respectively.

$$G_d(s) = \frac{1}{r_s + s L_d} \quad (33)$$

$$G_q(s) = \frac{1}{r_s + s L_q} \quad (34)$$

To start with the H_{∞} design, let's consider the block scheme of the configuration in Fig.5, where G(s) represents the transfer function of the plant. K(s) is the controller to be designed. The control objective is to make the output i_0 follow the reference, i_{ref} , as closely as possible.

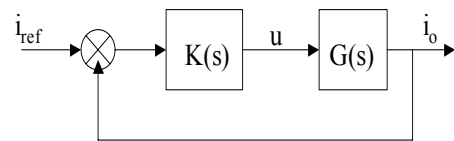


Fig. 5 Feedback configuration

Using the system in Fig.5, we have,

- For the feedback configuration in the d axis:

$$i_0(t) = i_d(t), \\ i_{ref} = i_{dr}, \\ G(s) = G_d(s), \\ K(s) = K_d(s)$$

- For the feedback configuration in the q axis:

$$i_0(t) = i_q(t), \\ i_{ref} = i_{qr}, \\ G(s) = G_q(s), \\ K(s) = K_q(s)$$

Remark: In Fig.5, Only the systems G_d and G_q are considered because the static gain of the inverter is taken equal to 1, saturations, voltage drops and delays due to the inverter are neglected .

By incorporating weighting filters to output signals e , u , and i_0 in the closed-loop configuration of Fig. 5, we obtain the configuration diagram of Fig. 6. The error e is weighted by the filter $w_1(s)$, the command u by $w_2(s)$, and the output i_0 by $w_3(s)$.

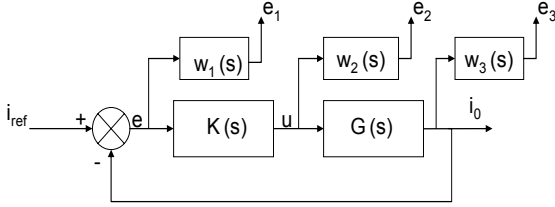


Fig. 6 Introduction of weighting filters

$$e_1(s) = w_1(s) S(s) i_{ref}(s) \quad (35)$$

$$e_2(s) = w_2(s) K_q(s) S(s) i_{ref}(s) \quad (36)$$

$$e_3(s) = w_3(s) G_q(s) K_q(s) S(s) i_{ref}(s) \quad (37)$$

$$S(s) = (1 + GK)^{-1} \quad (38)$$

$$T(s) = GK S \quad (39)$$

$S(s)$ and $T(s)$ are respectively the sensitivity and the complementary sensitivity functions. Let γ be chosen as 1. The H_∞ control design will be formulated in such a way that an optimal controller will be designed such that the closed-loop transfer function satisfies the infinity-norm inequality:

$$\|T_z w\|_\infty = \left\| \begin{array}{c} w_1 S \\ w_2 K S \\ w_3 T \end{array} \right\|_\infty < 1 \quad (40)$$

The inequality (40) implies that

$$\forall \omega \in R \quad |S(j\omega)| < \frac{1}{|w_1(j\omega)|} \quad (41)$$

$$\forall \omega \in R \quad |K(j\omega)S(j\omega)| < \frac{1}{|w_2(j\omega)|} \quad (42)$$

$$\forall \omega \in R \quad |T(j\omega)| < \frac{1}{|w_3(j\omega)|} \quad (43)$$

The selection of the weighting filters for the feedback configuration in the q axis is as follows:

The filter $w_1(s)$ was selected so that the Bode diagram of $1/|w_1(j\omega)|$:

1. intercepts the 0-dB axis at the frequency 156 rad/s so that the open-loop transfer function bandwidth will be close to 156 rad/s,

2. presents a gain of 1.51 at high frequencies in order to limit the H_∞ norm of the sensitivity S . This imposes a stability margin of at least 0.66.
3. allows the tracking of the reference input by the output with a static error less than 0.01%.

$$w_1(s) = \frac{1}{1.51} \frac{(s + 177.3493)}{(s + 0.0117)} \quad (44)$$

The control weighting function $w_2(s)$ is chosen simply as the scalar function:

$$w_2(s) = 0.5 \frac{1 + 10^{-3}s}{1 + 210^{-5}s} \quad (45)$$

The filter w_3 is selected so that the gain of $1/|w_3|$ is 6 dB at low frequencies and the attenuation is 80 dB at high frequencies. The frequency at which the Bode diagram of $1/|w_3|$ intercepts the 0-dB axis is 235 rad/s.

$$w_3(s) = 10^4 \frac{s + 135.68}{s + 271.35 \cdot 10^4} \quad (46)$$

The weighting filters for the feedback configuration in the d axis are:

$$w_1(s) = \frac{1}{1.7} \frac{s + 68.7386}{s + 0.0040} \quad (47)$$

$$w_2(s) = 25 \frac{s + 1000}{s + 50000} \quad (48)$$

$$w_3(s) = 10^4 \frac{s + 577.3503}{s + 1.1547 \cdot 10^7} \quad (49)$$

3.3. Design of the controller K_q

Comparison between the block diagrams of Fig.1 and Fig.6 gives:

- Inputs: $w(t) = i_{qr}(t)$

- Supervised signals: $z(t) = [e_1(t) \ e_2(t) \ e_3(t)]^T$

- Input of the controller: $y(t) = e(t)$

- The controller output is $u(t)$ in Fig.1 and Fig.6.

The representation (1) used to solve the H_∞ problem is obtained by considering a state representation for each of the following transfer functions $G_q(s)$, $w_1(s)$, $w_2(s)$, and $w_3(s)$:

$G_q(s)$: (input u , output i_q):

$$\begin{aligned} \dot{x}_1 &= -214.2857 x_1 + u \\ i_q &= 357.1429 x_1 + 0u \end{aligned} \quad (50)$$

$w_1(s)$: (input e , output e_1):

$$\begin{aligned} \dot{x}_2 &= -0.0117 x_2 + e \\ e_1 &= 117.4421 x_2 + 0.6623 e \end{aligned} \quad (51)$$

$w_2(s)$: (input u , output e_2):

$$\begin{aligned} \dot{x}_3 &= -510^4 x_3 + u \\ e_2 &= 1.22510^6 x_3 + 25u \end{aligned} \quad (52)$$

$w_3(s)$: (input i_q , output e_3):

$$\begin{aligned} \dot{x}_4 &= -271.3546 x_4 + i_q \\ e_3 &= 271.341010^8 x_4 + 10^4 i_q \end{aligned} \quad (53)$$

The error $e(t)$ and the state vector $x(t)$ are:

$$e(t) = i_{qr}(t) - i_q(t) \quad (54)$$

$$x = [x_1 \ x_2 \ x_3 \ x_4]^T \quad (55)$$

Finally, we get the state representation (1) from the above equations. The matrices A , B_1 , B_2 , C_1 , D_{11} , D_{12} , C_2 , D_{21} , D_{22} are given as follows:

$$A = \begin{bmatrix} -214.2857 & 0 & 0 & 0 \\ -357.1428 & -0.0117 & 0 & 0 \\ 0 & 0 & -510^4 & 0 \\ 357.1428 & 0 & 0 & -271.354610^4 \end{bmatrix} \quad (56)$$

$$B_1 = [0 \ 1 \ 0 \ 0]^T \quad (57)$$

$$B_2 = [1 \ 0 \ 1 \ 0]^T \quad (58)$$

$$C_1 = \begin{bmatrix} -236.5184 & -117.4421 & 0 & 0 \\ 0 & 0 & -1225 \cdot 10^3 & 0 \\ 357.1429 \cdot 10^4 & 0 & 0 & -2.7134 \cdot 10^{10} \end{bmatrix} \quad (59)$$

$$D_{11} = [0.6623 \ 0 \ 0]^T \quad (60)$$

$$D_{12} = [0 \ 25 \ 0]^T \quad (61)$$

$$C_2 = [-357.1429 \ 0 \ 0 \ 0] \quad (62)$$

$$D_{21} = 1 \quad D_{22} = 0 \quad (63)$$

$$\begin{bmatrix} \dot{x}(t) \\ z(t) \\ y(t) \end{bmatrix} = \begin{bmatrix} A & B_1 & B_2 \\ C_1 & D_{11} & D_{12} \\ C_2 & D_{21} & D_{22} \end{bmatrix} \begin{bmatrix} x(t) \\ i_{qr}(t) \\ u(t) \end{bmatrix} \quad (64)$$

The system data given is not in the normalisation form. In order to apply theorem 1, certain transformations must be used first. Using the singular value decomposition (SVD), we find orthogonal matrices U_{12} , and V_{12} such that

$$U_{12} D_{12} V_{12}^T = \begin{bmatrix} 0 \\ \Sigma_{12} \end{bmatrix} \quad (65)$$

$$U_{12} D_{12} V_{12}^T \Sigma_{12}^{-1} = [0 \ 0 \ 1]^T \quad (66)$$

$$U_{12} = \begin{bmatrix} -1 & 0 & 0 \\ 0 & 0 & 1 \\ 0 & -1 & 0 \end{bmatrix} \quad V_{12} = -1 \quad \Sigma_{12} = 25$$

$$U_{12} = \begin{bmatrix} U_{121} \\ U_{122} \end{bmatrix} \quad U_{121} = \begin{bmatrix} -1 & 0 & 0 \\ 0 & 0 & 1 \end{bmatrix}$$

$$U_{122} = [0 \ -1 \ 0]$$

The orthogonal transformation on D_{21} is not needed since $p_2 = m_1$ and $p_1 > m_2$.

The normalisation of $P(s)$ into $\bar{P}(s)$ is based on the above transformations, and is obtained as follows:

$$\begin{aligned} \bar{B}_1 &= B_1 \\ \bar{B}_2 &= B_2 V_{12}^T \Sigma_{12}^{-1} \\ \bar{C}_1 &= U_{12} C_1 \\ \bar{C}_2 &= C_2 \\ \bar{D}_{11} &= U_{12} D_{11} \\ \bar{D}_{12} &= U_{12} D_{12} V_{12}^T \Sigma_{12}^{-1} = [0 \ 0 \ 1]^T \\ \bar{D}_{21} &= D_{21} \end{aligned} \quad (67)$$

\bar{D}_{11} can be partitioned as follows:

$$\bar{D}_{11} = \begin{bmatrix} \bar{D}_{1111} & \bar{D}_{1112} \\ \bar{D}_{1121} & \bar{D}_{1122} \end{bmatrix}$$

$$\bar{D}_{1112} = [-0.6623 \ 0]^T \quad \bar{D}_{1122} = 0$$

$$B = [\bar{B}_1 \ \bar{B}_2]$$

$$C = [\bar{C}_1^T \ \bar{C}_2^T]^T$$

In order to apply theorem 1, the matrices in the general form (matrices without bars) of $P(s)$, used in section (3.1), are replaced by matrices in the normalized system data $\bar{P}(s)$ (matrices with bars). $\bar{P}(s)$ is the normalised system in the q axis.

The first condition of theorem 1 is satisfied since we have:

$$\max(\bar{\sigma}[D_{1111} \ D_{1112}], \bar{\sigma}([D_{1111}^T \ D_{1121}^T]^T)) = 0.6623 < 1$$

Matrices R_{nh} and R_{nj} are given by equations (14) and (15), respectively.

$$R_{nh} = \begin{bmatrix} -0.5614 & 0 \\ 0 & 1 \end{bmatrix}$$

$$R_{nj} = \begin{bmatrix} -0.5614 & 0 & 0 & -0.6623 \\ 0 & -1 & 0 & 0 \\ 0 & 0 & -1 & 0 \\ -0.6623 & 0 & 0 & 1 \end{bmatrix}$$

R_{nh} and R_{nj} are nonsingular. This condition implies the existence of the two Hamiltonian matrices H and J, given by equations (16) and (17).

The stabilising solution X that solves the Riccati equation (18) is denoted as

$$X = Ric \begin{bmatrix} E_x & -W_x \\ -Q_x & -E_x^T \end{bmatrix}$$

$$X = 10^4 \begin{bmatrix} 235.21 & -0.17 & 10.01 & -17.8410^5 \\ -0.17 & 0.08 & -2.92 & -33.24 \\ 10.01 & -2.92 & 203.22 & -29.9210^3 \\ -17.84210^4 & -33.24 & -29.92110^3 & 135.5610^8 \end{bmatrix}$$

The eigenvalues of the matrix X are:

$$\lambda_1 = 1.35561 \cdot 10^{14} \quad \lambda_2 = 203.3817 \cdot 10^4$$

$$\lambda_3 = 2508 \quad \lambda_4 = 1$$

X is positive definite.

The stabilising solution Y that solves the Riccati equation (19) is denoted as

$$Y = Ric \begin{bmatrix} E_y & -W_y \\ -Q_y & -E_y^T \end{bmatrix}$$

$$Y = \begin{bmatrix} 0 & 0 & 0 & 0 \\ 0 & 0 & 0 & 0 \\ 0 & 0 & 0 & 0 \\ 0 & 0 & 0 & 0 \end{bmatrix}$$

The eigenvalues of the matrix Y are:

$$\lambda_1 = \lambda_2 = \lambda_3 = \lambda_4 = 0$$

The matrix Y is positive semi definite.

The eigenvalues of the matrix $E_x - W_x X$ are

$$\lambda_1 = -2.7173 \cdot 10^6 \quad \lambda_2 = -167.4581 + j65.6802$$

$$\lambda_3 = -167.4581 - j65.6802 \quad \lambda_4 = -2807.3204$$

The eigenvalues of the matrix $E_y - W_y Y$ are

$$\lambda_1 = -214.2857 \quad \lambda_2 = -0.0117$$

$$\lambda_3 = -50000 \quad \lambda_4 = -271.3546 \cdot 10^4$$

The matrices $E_x - W_x X$ and $E_y - W_y Y$ are stable since the real parts of their corresponding eigenvalues are negative.

The spectral radius is

$$\rho(XY) = 0 < 1 \quad (\gamma^2 = 1).$$

The conditions of theorem 1 are satisfied, then the controller K_q is computed by applying theorem 2.

By using equations (20) through (32), we obtain the the following results:

$$\hat{D}_{11} = -\bar{D}_{1121} \bar{D}_{1111}^T T D_{11} - \bar{D}_{1122} = 0$$

$$T_1 = I_{m_2} - \bar{D}_{1112} T D_{12} \bar{D}_{1121}^T \quad T_2 = T_1^T = 1$$

$$\hat{D}_{12} \text{ is the Cholesky factor of } T_2: \hat{D}_{12} = 1$$

$$T_3 = I_{p_2} - \bar{D}_{1112}^T T D_{21} \bar{D}_{1112} = 0.5614$$

$$\hat{D}_{21} \text{ is the Cholesky factor of } T_3: \hat{D}_{21} = 0.7493$$

$$Z = (I_4 - \gamma^{-2} Y X)^{-1} = \begin{bmatrix} 1 & 0 & 0 & 0 \\ 0 & 1 & 0 & 0 \\ 0 & 0 & 1 & 0 \\ 0 & 0 & 0 & 1 \end{bmatrix}$$

$$\hat{B}_2 = Z(\bar{B}_2 + L_{12}) \hat{D}_{12} = [-0.04 \quad 0 \quad -0.04 \quad 0]^T$$

$$\hat{C}_2 = -\hat{D}_{12}(\bar{C}_2 + F_{12})$$

$$\hat{C}_2 = 10^4 [0.3795 \quad -0.1650 \quad 5.2171 \quad 59.2236]$$

$$\hat{B}_1 = -Z L_2 + \hat{B}_2 \hat{D}_{12}^{-1} \hat{D}_{11} = [0 \quad 1 \quad 0 \quad 0]^T$$

$$\hat{C}_1 = U_{12}(F_2 + \hat{D}_{11} \hat{D}_{21}^{-1} \hat{C}_2)$$

$$\hat{C}_1 = 10^4 [-0.3923 \quad 0.0049 \quad 4.5588 \quad 2902.6445]$$

$$\hat{A} = A + B F + \hat{B}_1 \hat{D}_{21}^{-1} \hat{C}_2$$

$$\hat{A} = 10^4 \begin{bmatrix} -0.4137 & 0.0049 & 4.5588 & 2902.6445 \\ 0 & -1.1745 \cdot 10^{-6} & 0 & 0 \\ -0.3923 & 0.0049 & -0.4411 & 2902.6445 \\ 0.0357 & 0 & 0 & -271.3546 \end{bmatrix}$$

The suboptimal controller called the central controller is given in state-space form:

$$K_q(s) = K(s) = \begin{bmatrix} \hat{A} & \hat{B}_1 \\ \hat{C}_1 & \hat{D}_{11} \end{bmatrix}$$

The corresponding transfer function is given by

$$K_q(s) = \frac{49.70(s + 2.714 \cdot 10^6)(s + 510^4)(s + 214.3)}{(s + 2.71710^6)(s + 0.01174)(s^2 + 4793s + 6.10410^6)} \quad (68)$$

The open-loop transfer function L(s) is given by equation (69).

$$L(s) = G_q(s) K_q(s) \quad (69)$$

The frequency response of L(s) is shown in Fig.7. The gain margin is 31.2 dB, it occurs at the frequency 2600 rad/s. The phase margin is 83.7 degrees, and it occurs at 145 rad/s. The stability margin M_m is

$$M_m = \inf \{ |1 + L(j\omega)| / \omega \text{ varies} \} = \frac{1}{\|S\|_\infty} = 0.92$$

The steady state error is given by:

$$e_{ss} = \frac{1}{1 + \lim_{s \rightarrow 0} (L(s))} = 8 \cdot 10^{-5} < 10^{-4}$$

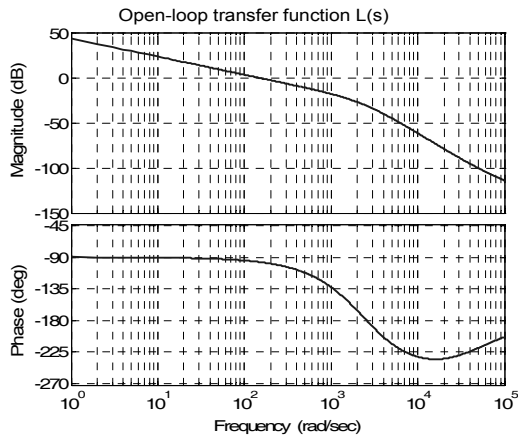


Fig. 7 Frequency response of (L(s))

The transient response to reference input i_{qr} , is given in Fig.8, the settling time is 0.025 second, and the rise time is 0.013 second, the maximum overshoot is 0%.

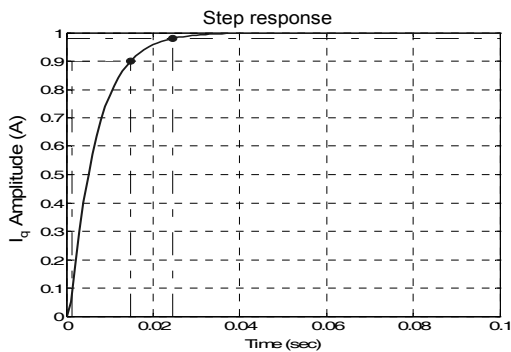


Fig. 8 Transient response to reference input

The conditions 41, 42, and 43 are satisfied as shown in figures 9, 10, and 11 respectively.

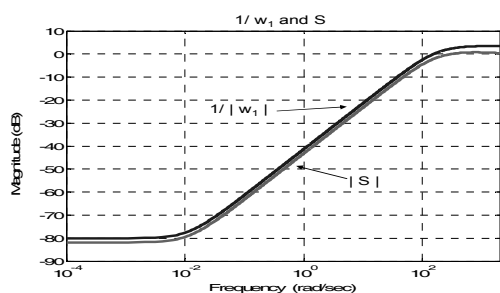


Fig. 9 |S| and its bound 1/|w1|

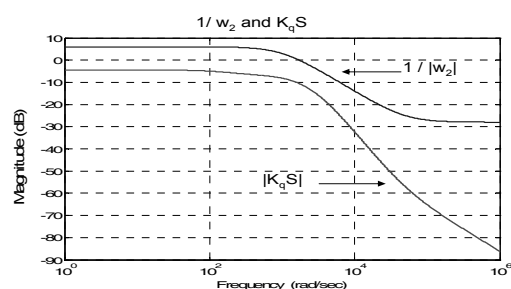


Fig. 10 |K_qS| and its bound 1/|w₂|

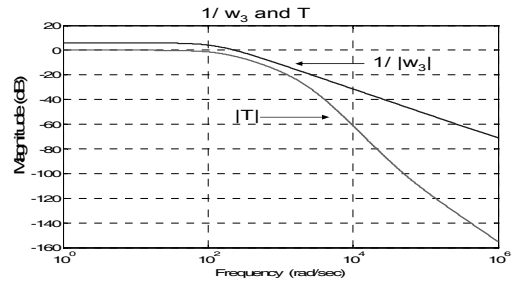


Fig. 11 |T| and its bound 1/|w₃|

3.4. Design of the controller K_d

The controller K_d is designed by applying the same procedure as in section (3.3). The data is taken from the plant in the d axis; this consists of the system $G_d(s)$ and the weighting filters $w_1(s)$, $w_2(s)$ and $w_3(s)$ given by equations (24), (25) and (26) respectively. The transfer function $K_d(s)$ has been computed. It is given by:

$$K_d = \frac{2.7364(s + 1.15510^6)(s + 510^4)(s + 428.6)}{(s + 1.15510^6)(s + 0.0040)(s^2 + 2428s + 1.58410^6)} \quad (70)$$

The system with K_d achieves the following performances:

- In the frequency domain, the gain margin is 32.3 dB, it occurs at 1290 rad/sec. The phase margin is 84.7 degrees, it occurs at 61 rad/sec.
- In the time domain, the settling time is 0.059 second, and the rise time is 0.032 second.

The steady state error is given by:

$$e_{ss} = \frac{1}{1 + \lim_{s \rightarrow 0} (L(s))} = 6.610^{-5}$$

The stability margin M_m is

$$M_m = \inf\{ |1 + L(j\omega)| \mid \omega \text{ varies} \} = \frac{1}{\|S\|_{\infty}} = 0.95$$

3.5. Controller-order reduction

The order of the controllers K_q and K_d can be reduced to the third order. The transfer functions become:

$$K_{qr} = 49.7026 \frac{(s + 5 \cdot 10^4)(s + 214.3)}{s(s^2 + 4793s + 6.104 \cdot 10^6)} \quad (71)$$

$$K_{dr} = \frac{2.7364 (s + 5 \cdot 10^4)(s + 428.6)}{s(s^2 + 2428s + 1.584 \cdot 10^6)} \quad (72)$$

4. SIMULATION RESULTS

In order to perform the simulation using the system of Fig.4, the speed controller is a PID controller with the following coefficients:

$$K_p = 0.5045, \quad K_D = 0.0045, \quad K_I = 0.5$$

The global system shown in Fig.4 is tested by numerical simulation. The input ω_{ref} is a step function with magnitude 175 rad/s. The mechanical torque applied to the motor's shaft is originally 0 Nm. First, we consider the nominal models in the d and q axes. Figure 12 shows that the electromagnetic torque climbs to nearly 14.3 Nm when the motor starts and stabilizes rapidly when the motor reaches the reference value. The mechanical torque steps to 3 Nm at instant $t = 0.08$ second. At this instant, the stator current i_q and the electromagnetic torque increase to maintain the speed at its reference value. Now, let the time constants of the plants vary by 50% of their nominal values, given below:

$$\tau_d = \frac{L_d}{r_s} = 2.3310^{-3} \text{ s}, \quad \tau_q = \frac{L_q}{r_s} = 4.6610^{-3} \text{ s}$$

Fig.13 shows that the electromagnetic torque T_e , the stator currents i_d and i_q produced, when the time constants vary, do not differ from those produced under the nominal plants.

The oscillations of the current at the point of a load-torque step in Fig.12 and Fig. 13 are due to the fact that the differentiator portion of the PID controller is a high-pass filter, which usually accentuates any higher frequency noise that enters the system.

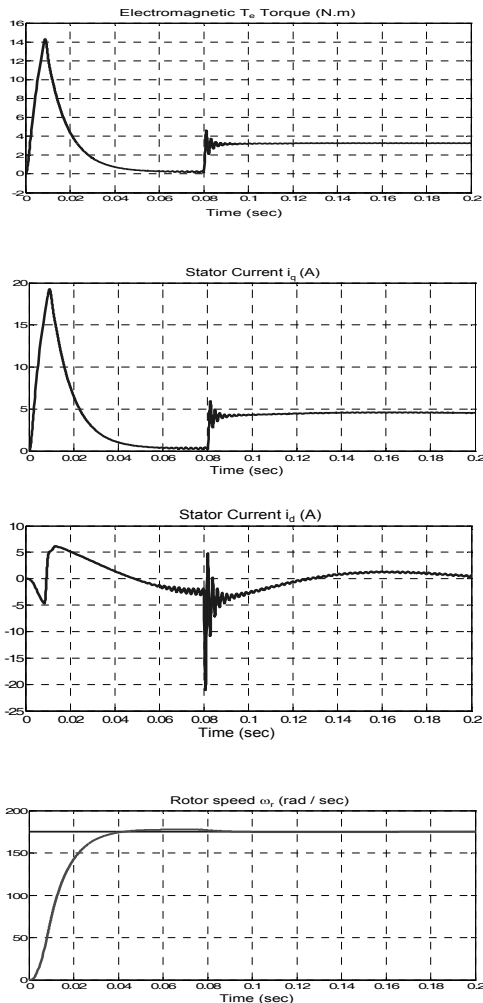


Fig. 12 Currents, torque and speed (nominal plants)

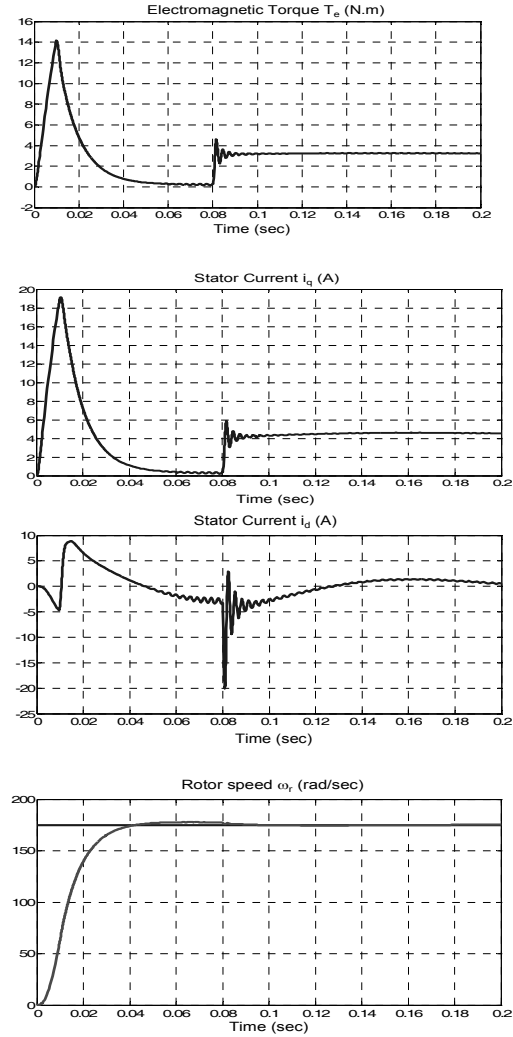


Fig. 13 Currents, torque and speed (variation of time constants)

5. CONCLUSION

The performance weighting function $w_1(s)$ ensures the following performances:

- Good transient response; with the K_d controller, the settling time is 0.059 sec and with the K_q controller, the settling time is 0.025 sec. The difference is due to the fact that the bandwidth of the system with K_d is 50 rad/sec and that of the system with K_q is 145 rad/sec. A larger bandwidth gives rise to a faster settling time.
- The steady-state error with K_d is $6.6 \cdot 10^{-5}$, the steady-state error with K_q is $8 \cdot 10^{-5}$. Both errors are smaller than 10^{-4} .
- The stability margin which indicates the robustness of the closed-loop system against the errors of the model is 0.95 with K_d and 0.92 with K_q . Both margins are greater than 0.60 and 0.66.

The results suggest that the sensitivity S should be penalised heavily at low frequencies to achieve good reference tracking and performance robustness. According to the simulation, although the time constants of the models vary by 50%, the stability and performance are maintained within acceptable limits. The H_∞ design produces high-order controllers.

6. PARAMETERS OF THE PMSM MACHINE

The parameters of the PMS machine are:

$$L_d = 1.4 \text{ mH}, \quad L_q = 2.8 \text{ mH}, \quad r_s = 0.6 \Omega \quad I_{q \max} = 20 \text{ A}, \\ P = 4, \quad \phi_f = 0.12 \text{ Wb} \quad \omega_{rn} = 230 \text{ rad/s}, \quad T_m = 8.5 \text{ Nm} \\ J = 1.1110^{-3} \text{ Kg m}^2, \quad F = 1.410^{-3} \text{ Nm/rds}^{-1}.$$

REFERENCES

- [1] Doyle J. Glover, K. Khargonekar, P. and Francis, B : "State-space solutions to standard H_2 and H_∞ control problems," IEEE Trans. Automat. Contr., AC-34, no. 8, pp. 831-847, Aug. 1989.
- [2] Duc, G. Font, S : *Commande H_∞ et μ -analyse, Des outils pour la robustesse*, HERMES Science Publications, Paris, 1999.
- [3] Glover, K. and Doyle, J. C : "State Space Formulae for All Stabilizing Controllers that Satisfy an H_∞ -Norm Bound and Relations to Risk Sensitivity", Systems and Control Letters, 1988
- [4] Khargonekar, P. P. Petersen, I. R. and Rotea, M. A. : "H ∞ optimal control with state feedback," IEEE Trans. Automat. Contr., AC-33, pp. 783-786, 1988.
- [8] D.J.N. Limebeer and E. Kasenally, unpublished notes, 1987.
- [5] Petkov, D.-W. Gu, P. Hr. and Konstantinov, M.M: *Robust Control Design with MATLAB*, Springer-Verlag London 2005.
- [6] Stoorvogel, A.A: *The H_∞ Control Problem: A state Space Approach*, Prentice Hall, Englewood Cliffs, NJ, 1992.
- [7] STURTZER, G. SMIGIEL E: *Modélisation et commande des moteurs triphasés*, Ellipses, 2000.
- [8] Zhou, K. Doyle, J.C. and Glover, K: *robust and optimal control*, Prentice Hall, Upper Saddle River, NJ, 1995.

Received Jun 26, 2006, accepted Jun 15, 2007

BIOGRAPHIES

Ahmed Azaiz was born in 1956 in Mascara Algeria. He received his BS degree in electrical engineering, computer option from the Institute of Electricity and Electronics Institute (INELEC) Boumerdes in 1988 and the MS degree in Electronics from the University of Sidi Bel Abbes in 1993. He is currently professor of Electronics at the University of Sidi Bel Abbes. His research interests are on microprocessor systems and robust control.

Youcef Ramdani was born in 1952 in Sidi Bel Abbes Algeria. He received his BS degree in electrical engineering from USTO University in 1978, DEA in Electronics from Bordeaux, France in 1986, PhD in electrical engineering from the Faculty of sciences of the University of Bordeaux, France, in 1989. He is currently Professor of electrical engineering at the University of Sidi Bel Abbes.

Abdelkader Meroufel was born in 1954 in Sidi Bel Abbes Algeria. He received his BS degree in electrical engineering from USTO University in 1979, the MS degree from USTO University (Algeria) in 1990, and the PhD degree from the University of Sidi Bel Abbes in 2004. He is currently Professor of electrical engineering at the University of Sidi Bel Abbes.

Baghdad Bel Abbes was born in 1952 in Sidi Bel Abbes Algeria. He received his BS degree in electrical engineering from the electrical engineering Institute of Annaba in 1976 and the MS degree from the University of Sidi Bel Abbes in 2002. He is currently Professor of electrical engineering at the University of Sidi Bel Abbes.